ORIGINAL RESEARCH

Laryngoscope
Investigative Otolaryngology

Diagnostic usefulness of cone-beam computed tomography versus multi-detector computed tomography for sinonasal structure evaluation

Miran Han MD[1,2] 🄳 | **Hyun Jun Kim MD, PhD[3]** 🄳 | **Jin Wook Choi MD, PhD[1]** |
Do-Yang Park MD, PhD[3] | **Jang Gyu Han MD[3]**

[1]Department of Radiology, Ajou University Hospital, Ajou University School of Medicine, Suwon, Republic of Korea

[2]Department of Radiology, Graduate School of Kangwon National University, Chuncheon, Republic of Korea

[3]Department of Otolaryngology, Ajou University Hospital, Ajou University School of Medicine, Suwon, Republic of Korea

Correspondence
Hyun Jun Kim, Department of Otolaryngology, Ajou University Hospital, Ajou University School of Medicine, 164, World Cup-ro, Yeongtong-gu, Suwon 16499, Republic of Korea.
Email: entkhj@ajou.ac.kr

Funding information
National Research Foundation of Korea, Grant/Award Number: NRF-2021R1H1A2093767

Abstract

Objective: Cone-beam computed tomography (CBCT) is a promising imaging modality for sinonasal evaluation, with advantages of relatively low radiation dose, low cost, and quick outpatient imaging. Our study aimed to compare the diagnostic performance and image quality of CBCT with those of multi-detector computed tomography (MDCT) with different slice thickness.

Methods: We retrospectively reviewed 60 consecutive patients who had undergone both CBCT and MDCT. MDCT images was reconstructed with 1 and 3 mm slice thickness. The quantitative image quality parameters (image noise, signal-to-noise ratio [SNR], and contrast-to noise ratio [CNR] were calculated and compared between the two imaging modalities. Two observers (ENT surgeon and neuroradiologist) evaluated the presence of seven sinonasal anatomic variations in each patient and interobserver agreements were analyzed. The diagnostic performance of CBCT (0.3 mm) and MDCT (3 mm) was assessed and compared with that of high resolution MDCT (1 mm), which is considered as the gold standard.

Results: The image noise was significantly higher and SNR and CNR values were lower in the CBCT (0.3 mm) group than in the MDCT groups (1 and 3 mm). The diagnostic performance of CBCT (0.3 mm) was similar to that of MDCT (1 mm) and superior to that of MDCT (3 mm). The highest interobserver agreement was for high resolution MDCT (1 mm), followed by CBCT (0.3 mm), and MDCT (3 mm).

Conclusion: Considering its low radiation dose, low cost, and ease of clinical access, CBCT may be a useful imaging modality for as first line sinonasal evaluation and repeated follow up.

Study design: Retrospective study in a tertiary referral university center.

Level of evidence: NA.

1 | INTRODUCTION

Cone-beam computed tomography (CBCT), a radiographic imaging technique that has been in use since the 2000s, was initially developed for angiography; however, its recent applications include image-guided radiation therapy, surgical planning, and intraoperative imaging.[1–4] Currently, CBCT is most widely used in dentistry for dentomaxillofacial imaging, with increasing applications in otorhinolaryngology for the evaluation of the sinuses and temporal bone.[5–10]

The CBCT scanner uses a source of cone-shaped x-ray beam and a two-dimensional plane detector, which is fixed to a rotating gantry. The gantry completes a partial or complete rotation around the region of interest (the patient's head), with the cone-shaped x-ray beam directed toward the plane detector on the opposite side. Several projection images of the field of view are acquired during the rotation, each covering the field of view from a different horizontal angle. A single rotation of the gantry allows acquisition of an entire volumetric dataset. Conversely, MDCT uses a fan-shaped x-ray beam with simultaneous translation of the gantry along with rotation of the x-ray source and detector. Several individual image slices of the field of view are acquired, which are then stacked to obtain a three-dimensional image reconstruction. The raw projection images in CBCT are composed of isotropic voxels; in contrast, the images in conventional multi-detector computed tomography (MDCT) are composed of anisotropic voxels.[11,12] Isotropic voxels allow high-fidelity image reconstruction in any plane, which is a major advantage of CBCT over MDCT. Moreover, the radiation dose used in CBCT is much lower than that used in MDCT,[13–15] and the compact design and low cost of CBCT scanners facilitate its clinical applications.

Chronic rhinosinusitis is a common and frequently recurrent disorder.[16] CT has become the method of choice for the diagnosis of rhinosinusitis and preoperative evaluation.[17–19] In 2017, the American College of Radiology reported about imaging considerations in various situation of sinonasal disease and CBCT was regarded as a reasonable option.[19] However, the report did not suggest practical imaging reformat thickness except imaging data within 2 mm for image-guided sinus surgery (IGSS). CBCT provides high spatial resolution images of the bone structure; however, its disadvantages include lack of soft-tissue contrast resolution and increased noise levels.[5,20] There exists an intrinsic trade-off between image noise and slice thickness in clinical CT imaging, regardless of beam shape. A thick slice is reconstructed with more x-ray photons, so it has lower image noise than thin slice image. Since more radiation is required to obtain low-noise images with thin slices, it is important to adjust the parameters with balance among radiation dose, image noise and slice thickness according to the clinical purpose.[21]

In this study, we aimed to evaluate the diagnostic performance of CBCT and MDCT with different slice thickness and radiation dose for the identification of sinonasal structures. Previous comparison studies[14,22–24] between CBCT and MDCT for sinonasal imaging had limitation, not comparing both images in the same patient. Our study had strength in that comparisons were conducted in a single study population.

2 | MATERIALS AND METHODS

2.1 | Patients and image acquisition

This study was approved by our Institutional Review Board and the requirement for written informed consent was waived due to its retrospective nature. All CT examinations included in this study were performed as standard-of-care procedures.

We retrospectively enrolled and reviewed 60 consecutive patients who had undergone both CBCT and MDCT within a 1-year period between March 2013 and December 2014 from our hospital patient's data base. The patients were transferred to the ear, nose, and throat department of our tertiary institution with clinical suspicion of a refractory sinonasal inflammatory disorder and with indication of surgical treatment. Patients initially received MDCT scan for preoperative evaluation. For patients who continued drug treatment, follow up CBCT was performed to evaluate treatment response. The exclusion criteria for the study subjects included history of sinonasal surgery, facial malformations, head-and-neck tumor, and dental restorations that could lead to poor image quality.

All CBCT examinations were performed on a single unit (DINNOVA, HDXWill, South Korea); the exposure parameters were as follows: tube voltage, 85 kV, and tube current, 7 mA. Slice thickness was 0.3 mm, with a maximum field of view (FOV) of 20 × 19 cm. MDCT examinations were performed using either the 128 channel (SOMATOM Definition Flash, Siemens, Germany) or 64 channel (Brilliance 64, Philips Healthcare, the Netherlands) scanner; the exposure and other parameters were as follows: tube voltage, 120 kV; tube current, 125 mA; FOV, 16 cm; pitch, 0.75; tube rotation time, 0.75 s; and collimation, 64 × 0.625 mm. The MDCT images were reconstructed with 1 and 3 mm slice thickness using a routine bone reconstruction algorithm. We selected MDCT slice thickness with 1 mm, which is generally recommended thickness for IGSS evaluation,[25,26] as a gold standard and with 3 mm, which is the thickest slice accepted for paranasal sinus evaluation in literature review.[17]

2.2 | Radiation dose analysis

The effective dose (ED) was estimated using dose-area-product (DAP) value[27,28] in CBCT and dose-length product (DLP) value based on computed tomography dose index-volume ($CTDI_{vol}$) in MDCT.

The DAP measurements were performed using a RaySafe X2 system (Unfors RaySafe, Sweden) according to the manufacturer manual. RaySafe X2 sensor was located at detector side and the DAP value was measured with same exposure parameters as the patient's protocol. Three times measurement were performed. The ED were calculated using conversion coefficient (E/DAP) of 0.17 μSv/mGy • cm^2 for large FOV in adult as follows[29]:

$$ED\,(\mu Sv) = DAP\,(mGy \bullet cm^2) \times E/DAP\,(\mu Sv/mGy \bullet cm^2).$$

The DLP values of each patient were obtained from picture archiving and communication systems (PACS) data. The ED were calculated using conversion factor (k) of 2.3 μSv/mGy • cm for head as follows[30,31]:

$$ED\,(\mu Sv) = DLP\,(mGy \bullet cm) \times k\,(\mu Sv/mGy \bullet cm).$$

2.3 | Image analysis

The quantitative image quality was compared using the following parameters: image noise (N), signal-to-noise ratio (SNR), and contrast-to-noise ratio (CNR). A neuroradiologist (M.H) placed the circular regions of interest (ROI) in the cortical bone of the zygomatic arch, pterygoid muscles, and air in the nasopharynx. The diameter of the ROI was made as large as possible depending on the anatomic region in each patient, same sized ROIs were placed at the same location for both CBCT and MDCT. Each measurement was calculated using the following definition and equation[30]:

Image noise (N): standard deviation of the ROI voxel values in the air.

A_b and A_m: mean attenuation of the ROI voxel values in the bone and muscle, respectively.

$SNR_b\,(bone) = A_b/N.$

$CNR_{b/m}\,(bone\ and\ muscle) = (A_b - A_m)/N.$

$CNR_{b/a}$ (bone and air) and $CNR_{m/a}$ (muscle and air) were calculated similarly.

A total of 120 bilateral sinonasal tracts from 60 patients were reviewed retrospectively. A neuroradiologist (M.H.) and an ENT surgeon (H.J.K.) recorded the presence of sinonasal anatomic variations in each patient on CBCT (0.3 mm) and MDCT (1 mm, 3 mm). They analyzed the images from each modality in separated session with a 2-week-interval. The presence of seven anatomic structures, namely septal deviation, Agger nasi cells, frontal cells, Haller cells, concha bullosa, Onodi cells, and lamina papyracea dehiscence, which are important anatomic variations for preoperative evaluation in endoscopic sinus surgery,[32,33] were independently evaluated by the two observers. Any discordance between the observers was resolved by consensus.

TABLE 2 Presence and detection rate of seven anatomic structures on each imaging modality

	CBCT (0.3 mm)	MDCT (1 mm)	MDCT (3 mm)
Septal deviation[a]	40 (66.7%)	40 (66. 7%)	40 (66.7%)
Agger nasi cell	103 (85.8%)	106 (88.3%)	101 (84.2%)
Frontal cell	87 (72.5%)	99 (82.5%)	68 (56.7%)
Haller cell	36 (30.0%)	50 (41.7%)	21 (17.5%)
Concha bullosa	49 (40.8%)	58 (48.3%)	41 (34.2%)
Onodi cell	47 (39.2%)	53 (44.2%)	38 (31.7%)
Lamina dehiscence	9 (7.5%)	7 (5.8%)	5 (4.2%)

Note: Total number of sinonasal tracts is 120, except.
Abbreviations: CBCT, cone-beam computed tomography; MDCT, multi-detector computed tomography.
[a]Total number of subjects is 60.

TABLE 1 Image noise, signal-to-noise ratio (SNR), and contrast-to-noise ratio (CNR) for each imaging method

	Noise[a]	SNR_b	$CNR_{b/m}$	$CNR_{b/a}$[a]	$CNR_{m/a}$[a]
CBCT (0.3 mm)	71.05 (15.15)	21.92 (5.83)	18.67 (5.61)	32.37 (7.66)	13.70 (2.80)
MDCT (1 mm)	58.61 (17.44)	24.55 (11.20)	23.56 (10.88)	42.86 (17.24)	19.30 (6.70)
MDCT (3 mm)	25.08 (8.14)	50.66 (19.09)	48.46 (18.60)	92.84 (30.13)	44.39 (12.51)
p value†	<.001*	<.001*	<.001*	<.001*	<.001*

Note: Data: mean (standard deviation). *p* value†: difference evaluated among MDCT (1 and 3 mm) and CBCT (0.3 mm) by ANOVA test. (CBCT [0.3 mm] vs. MDCT [1 mm], CBCT [0.3 mm] vs. MDCT [3 mm], MDCT [1 mm] vs. MDCT [3 mm]: *p* value <.05). SNR_b and $CNR_{b/m}$ showed significant difference between MDCT (1 mm) and MDCT (3 mm), between CBCT (0.3 mm) and MDCT (3 mm), but not between MDCT (1 mm) and CBCT (0.3 mm) on post hoc test.
Abbreviations: CBCT, cone-beam computed tomography; $CNR_{b/a}$, contrast between the bone and air; $CNR_{b/m}$, contrast between the bone and muscle; $CNR_{m/a}$, contrast between the muscle and air; MDCT, multi-detector computed tomography; SNR_b, SNR of the bone.
[a]Noise, $CNR_{b/a}$, $CNR_{m/a}$ showed significant difference between all subgroups on post hoc test.
*Statistically significant difference.

TABLE 3 Diagnostic performance of CBCT and MDCT for detecting sinonasal anatomic structures

		Sensitivity	Specificity	NPV	PPV	Accuracy	*p* value†	*p* value‡
Agger nasi cell	CBCT (0.3 mm)	96.2%	92.9%	76.5%	99.0%	95.8%	.38	.69
	MDCT (3 mm)	94.3%	92.9%	68.4%	99.0%	94.2%	.13	
Frontal cell	CBCT (0.3 mm)	87.9%	100.0%	63.6%	100.0%	90.0%	.001*	.001*
	MDCT (3 mm)	68.7%	100.0%	40.4%	100.0%	74.2%	<.001*	
Haller cell	CBCT (0.3 mm)	72.0%	100.0%	83.3%	100.0%	88.3%	<.001*	<.001*
	MDCT (3 mm)	42.9%	100.0%	71.7%	100.0%	76.7%	<.001*	
Concha bullosa	CBCT (0.3 mm)	82.8%	98.4%	85.9%	98.0%	90.8%	.01*	.10
	MDCT (3 mm)	70.7%	100.0%	78.5%	100.0%	85.8%	<.001*	
Onodi cell	CBCT (0.3 mm)	88.7%	100.0%	91.8%	100.0%	95.0%	.07	.01*
	MDCT (3 mm)	73.1%	100.0%	82.9%	100.0%	88.3%	<.001*	
Lamina dehiscence	CBCT (0.3 mm)	71.4%	96.5%	98.2%	55.6%	95.0%	.69	.22
	MDCT (3 mm)	57.1%	99.1%	97.4%	80.0%	96.7%	.63	

Note: Diagnostic performance was calculated based on the findings of MDCT (1 mm) considered as the gold standard. *p* value†, ‡ was evaluated with McNemar's test. *p* value†: difference evaluated with the gold standard imaging method, MDCT (1 mm). *p* value‡: difference evaluated between CBCT (0.3 mm) and MDCT (3 mm).

Abbreviations: CBCT, cone-beam computed tomography; MDCT, multi-detector computed tomography; NPV, negative predictive value; PPV, positive predictive value.

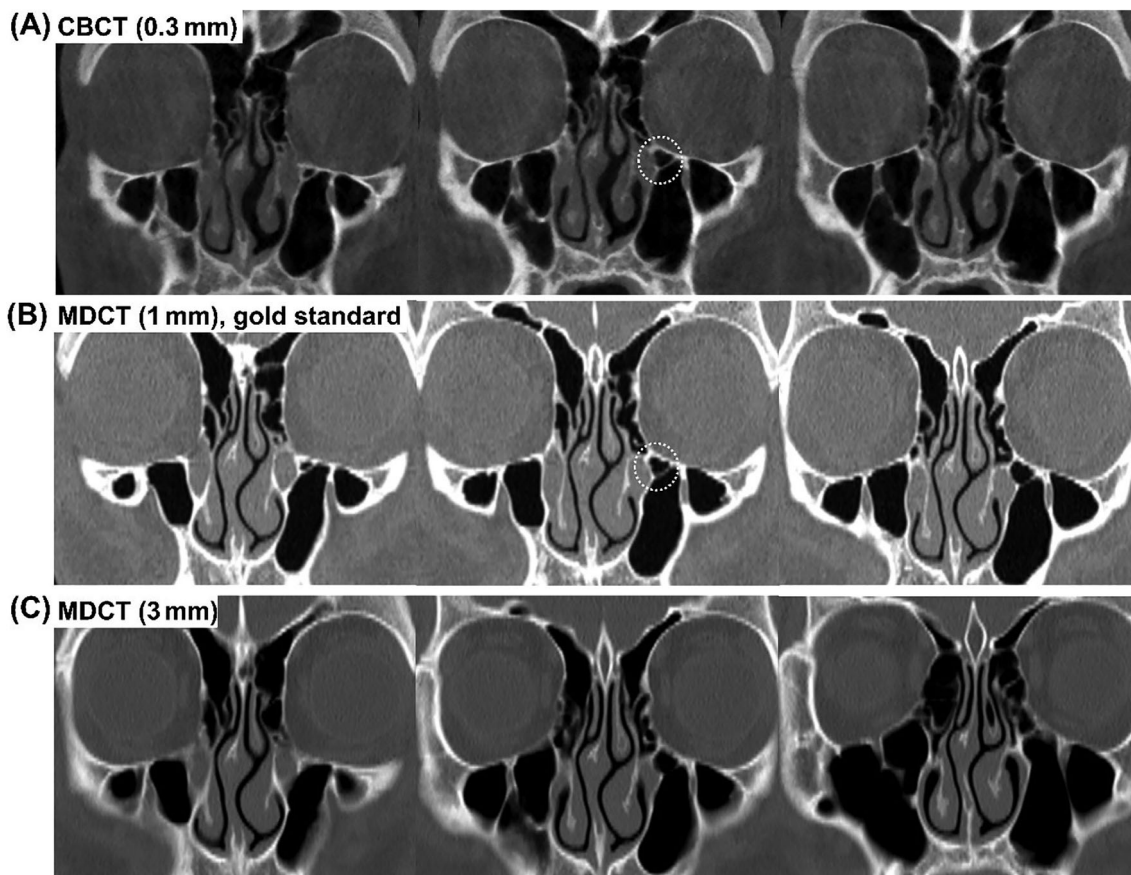*Statistically significant difference.

FIGURE 1   Haller cells (inside the dashed circle) on the left side are identified on (A) CBCT with 0.3 mm thickness and (B) MDCT with 1 mm thickness, but not on (C) MDCT with 3 mm thickness. CBCT, cone-beam computed tomography; MDCT, multi-detector computed tomography

FIGURE 2 Onodi cells (inside the dashed circle) on the right side are identified on (A) CBCT with 0.3 mm thickness and (B) MDCT with 1 mm thickness, but not on (C) MDCT with 3 mm thickness. CBCT, cone-beam computed tomography; MDCT, multi-detector computed tomography
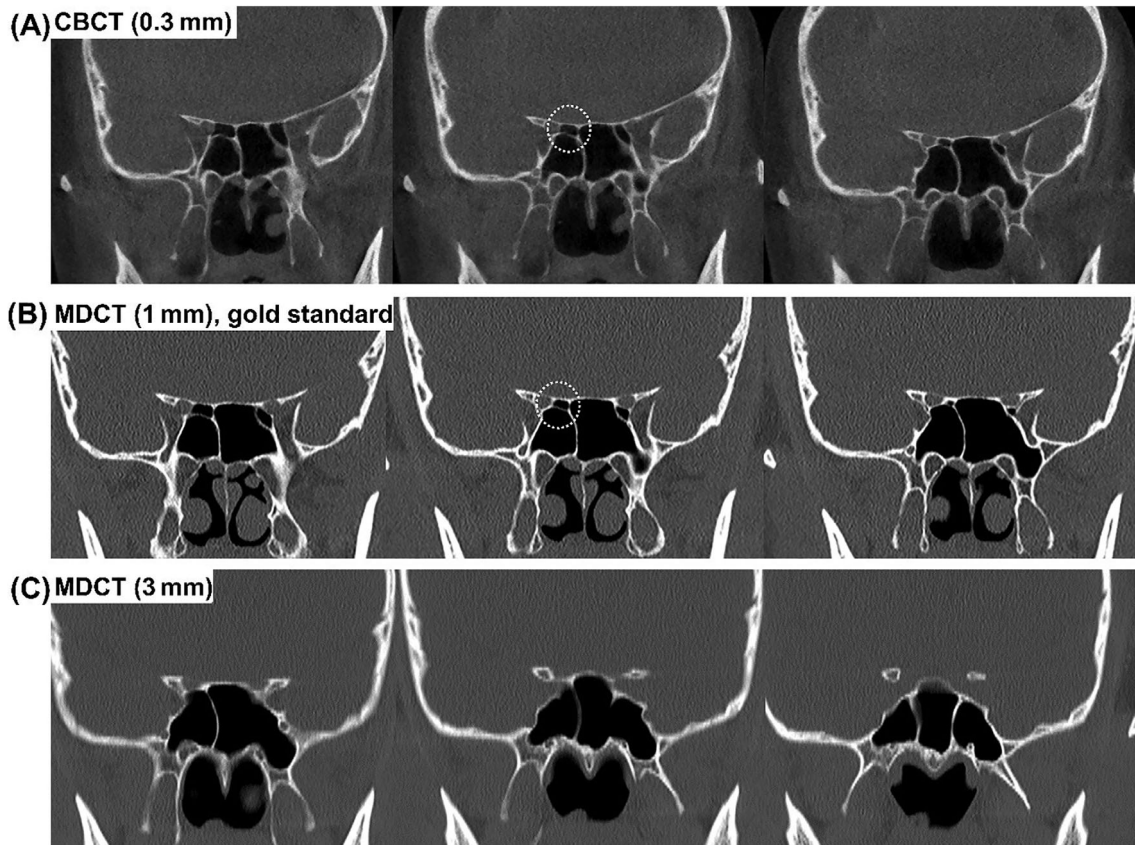
2.4 | Statistical analysis

The quantitative image quality for each imaging modality, represented by noise, SNR, and CNR, was compared using a one-way analysis of variance (ANOVA). The post hoc test for pairwise comparison of subgroups was performed using Tukey–Kramer test.

The diagnostic performance of both CBCT (0.3 mm) and MDCT with 3 mm thickness was evaluated based on the findings of MDCT with 1 mm thickness, which is considered as the gold standard. The sensitivity, specificity, negative predictive value (NPV), positive predictive value (PPV), and accuracy of detecting anatomic structures on CBCT (0.3 mm) and MDCT (3 mm) were calculated. The diagnostic performance of CBCT (0.3 mm) and MDCT (3 mm) was compared to that of standard MDCT (1 mm) for detecting the sinonasal anatomic structures, using the McNemar's test. The interobserver agreement was analyzed using the *Kappa* coefficient[34,35]: poor agreement <0.20; fair agreement: 0.21–0.40; moderate agreement: 0.41–0.60; substantial agreement: 0.61–0.80; and very good agreement: 0.81–1.0.

All statistical calculations were performed using the MedCalc statistical software (version 19, MedCalc, Ostend, Belgium); $p < .05$ was considered statistically significant.

3 | RESULTS

In total, 60 patients were included in this study; 36 patients (60%) were male and 24 (40%) were female. The mean age of the patients was 40.1 years (range, 11–67 years). The mean interval between the CBCT and MDCT scans for each patient was 3.0 months (standard deviation [SD], 2.9 months; range, 0.5–12 months). The mean effective radiation dose 271 μSv (SD, 0.15 μSv) for CBCT and 638.49 μSv (SD, 72.25 μSv) for MDCT. The ED of CBCT is approximately 57.4% lower compared with that of MDCT. The image noise in CBCT was significantly higher than that in MDCT ($p < .001$). The SNR (bone) and CNR (bone and muscle, bone and air, muscle and air) were the lowest in the CBCT (0.3 mm) group and highest in the MDCT (3 mm) group (Table 1). Image noise in CBCT (0.3 mm) was 17.5% higher compared to that in MDCT (1 mm) and 64.7% higher than that in MDCT (3 mm). The SNR (bone) and CNR (bone and muscle) of CBCT (0.3 mm) were significantly lower than those of MDCT (3 mm), but not significantly different from those of high resolution MDCT (1 mm).

The rate of presence of septal deviation, Agger nasi cells, frontal cells, Haller cells, concha bullosa, Onodi cells, and lamina papyracea dehiscence was 66.7%, 88.3%, 82.5%, 41.7%, 48.3%, 44.2%, and 5.8%, respectively (Table 2).
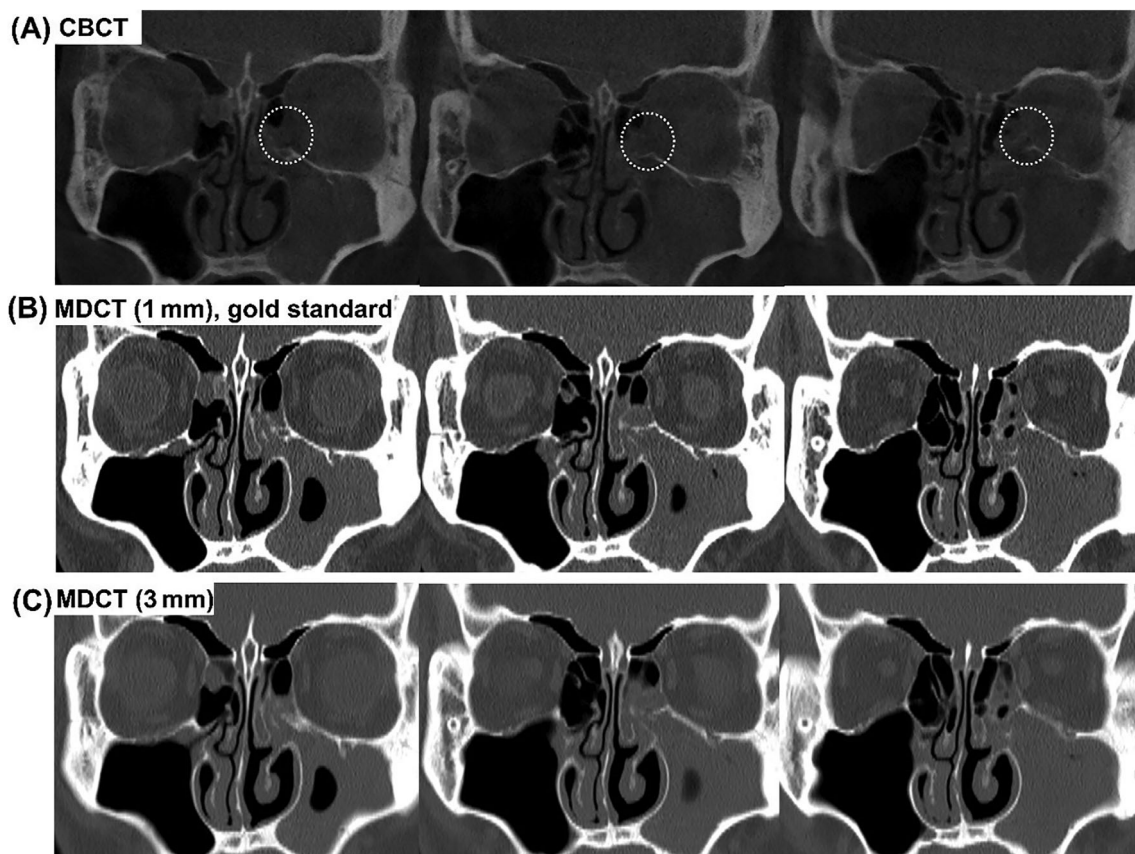
FIGURE 3   Lamina papyracea dehiscence (inside the dashed circle) is suspected on (A) CBCT with 0.3 mm thickness. However, an intact lamina papyracea is identified on MDCT with (B) 1 mm thickness and (C) 3 mm thickness. CBCT, cone-beam computed tomography; MDCT, multi-detector computed tomography

TABLE 4   Diagnostic concordance and interobserver agreement for anatomic structure evaluation

	Diagnostic concordance between reviewer 1 and 2			Agreement[a] between reviewer 1 and 2		
	CBCT (0.3 mm)	MDCT (1 mm)	MDCT (3 mm)	CBCT (0.3 mm)	MDCT (1 mm)	MDCT (3 mm)
Agger nasi cell	115 (95.8%)	116 (96.7%)	109 (90.8%)	0.80	0.81	0.69
Frontal cell	111 (92.5%)	117 (97.5%)	96 (80.0%)	0.79	0.88	0.62
Haller cell	113 (94.2%)	113 (94.2%)	115 (95.8%)	0.81	0.86	0.80
Concha bullosa	112 (93.3%)	113 (94.2%)	111 (92.5%)	0.86	0.88	0.83
Onodi cell	112 (93.3%)	112 (93.3%)	114 (95.0%)	0.86	0.86	0.86
Lamina dehiscence	113 (94.2%)	115 (95.8%)	117 (97.5%)	0.43	0.64	0.55

Note: *Kappa* value: Poor agreement <0.20; fair agreement, 0.21–0.40; moderate agreement, 0.41–0.60; substantial agreement, 0.61–0.80; very good agreement, 0.81–1.0.
Abbreviations: CBCT, cone-beam computed tomography; MDCT, multi-detector computed tomography.
[a]Agreement was evaluated using the *Kappa* coefficient.

The diagnostic performance of CBCT (0.3 mm) and MDCT (3 mm) for detecting anatomic structures is presented in Table 3. The overall diagnostic accuracy of CBCT (0.3 mm) was higher than that of MDCT (3 mm), and the difference was statistically significant for the detection of frontal cells, Haller cells, and Onodi cells (Figures 1 and 2). On the contrary, the diagnostic accuracy of CBCT (0.3 mm) was lower than that of MDCT (3 mm) for the detection of the lamina papyracea dehiscence only; however, the difference was not statistically significant. There were four false positive cases of lamina papyracea dehiscence in CBCT (0.3 mm) (Figure 3).

The interobserver agreements are presented as diagnostic concordance rates and *Kappa* coefficients in Table 4. The highest interobserver agreement was observed for high resolution MDCT (1 mm), followed by CBCT (0.3 mm) and MDCT (3 mm), except for the evaluation of lamina papyracea dehiscence. In case of septal deviation, two

observers showed consistent readings in both CBCT (0.3 mm) and MDCT (1 and 3 mm).

4 | DISCUSSION

In this study, we compared the diagnostic performance and quantitative image quality of CBCT (0.3 mm) with those of MDCT with different slice thickness (1 mm, 3 mm) in a single study population. CBCT showed similar diagnostic performance and observational variations compared to high resolution MDCT (1 mm), and superior performance compared to MDCT (3 mm) for detecting sinonasal anatomic variations; however, it showed increased image noise and lower SNR and CNR values.

CBCT showed lower objective image quality parameters (increased noise, and lower SNR and CNR) because image acquisition in CBCT was performed using a lower radiation dose and thinner slices (271 μSv [SD, 0.15 μSv], 85 kV, 8 mA, 0.3 mm slice thickness) compared to a higher radiation dose and thicker slices in MDCT (638.49 μSv [SD, 72.25 μSv], 120 kV, 125 mA, 1 and 3 mm slice thickness). Because the most important aim of diagnostic CT is the visual detection of the lesion, the image quality is determined based on the detectability of the scan, and not on the calculated metrics. In this respect, CBCT showed a similar performance to high resolution MDCT (1 mm) in detecting anatomic structures in the sinonasal cavity. The diagnostic performance of CBCT for detecting frontal cells, Haller cells, and the concha bullosa was significantly lower than that of high resolution MDCT (1 mm). However, the diagnostic performance of CBCT was superior to that of thick slice MDCT (3 mm), despite the higher SNR and CNR values, and lower image noise of MDCT (3 mm). The detectability of CBCT for Agger nasi cells and Onodi cells was similar to that of high resolution MDCT (1 mm). The interobserver agreement was the highest for high resolution MDCT (1 mm), followed by CBCT (0.3 mm), and MDCT (3 mm). The incidence of sinonasal anatomic variations in our study were comparable to that in previous reports.[32,33] Our result suggest that it would be better to focus on slice thickness rather than noise in sinonsal CT parameter selection. The CBCT with submillimeter slice could be more useful than thick slice thickness of MDCT in usual sinonasal evaluation.

The diagnostic accuracy of CBCT (0.3 mm) was lower than that of MDCT (3 mm) only in the detection of the lamina papyracea dehiscence, due to the four false positive cases in the CBCT arm. In these four cases, the normal lamina papyracea bony line was degraded and unidentifiable from the adjacent mucosal thickening (Figure 3). It may have been due to the lower SNR (bone) and CNR (bone and muscle) values in CBCT, resulting from the low radiation dose used. In a previous study,[24] low SNR and CNR values did not critically affect the depiction of normal anatomic structures surrounded by air; however, in patients with sinonasal polyposis, CBCT showed poor delineation between the margins of the bone and the soft tissue lesion due to reduction of contrast resolution by pathological soft tissue. This limitation should be considered during the interpretation of CBCT images. Because of the inadequate soft tissue contrast resolution of CBCT, its use should be limited in immunocompromised patients who are at a risk of developing invasive fungal sinusitis or sinusitis complications such as intracranial or periorbital abscesses.[36,37] Careful consideration should also be focused on CBCT scanning in elderly patients who may have accompanied sinonasal tumors in addition to inflammation.[38]

The effective dose of CBCT in our study was estimated approximately 57.4% lower than that of MDCT, as similar with previous studies.[14,15,24,39] Since chronic rhinosinusitis is particularly prevalent in children and adolescents, radiation exposure may be a more significant parameter in these patient groups. Additionally, chronic rhinosinusitis requires repeat assessment for serial follow-up after medical treatment or surgery, which makes radiation exposure in the patients a considerable issue.[16,40] Therefore, CBCT may be considered as a first-line imaging modality for the evaluation of sinonasal disease and repeated follow up imaging modalities, given the lower radiation dose. CBCT is particularly useful for evaluating the isolated ethmoid or sphenoid sinus lesions, which cannot be appropriately evaluated using plain radiography. However, despite the small voxel size of submillimeter, it showed inferior diagnostic performance than that of high resolution MDCT (1 mm) in some anatomic structures. Therefore, its use in operative candidates could not be strongly suggested.

In terms of cost, conventional MDCT for sinus evaluation costs three to five times more than CBCT.[30,41] Moreover, CBCT has a compact design and does not take up much space, which makes it accessible for use in local and primary care clinics. This, in turn, could potentially reduce the overall medical care costs.[42,43] Furthermore, claustrophobic and pediatric patients may prefer the open, sit-down format of CBCT over MDCT, which requires the patient to be placed inside the gantry in a supine position.[44]

This study had several limitations. First, it was performed in a single institution using a single CBCT unit. Due to large variations in CBCT radiation doses and image quality,[15,45] the findings of a single institution study cannot be generalized. Second, there was an examination interval (3.8 ± 5.9 months) between CBCT and MDCT scans of the patients. Any change in mucosal thickening and sinus inflammatory status may have affected image interpretation and anatomic variation detectability. However, this examination interval was essential[46] since it is unethical to expose patients to excessive radiation through repeat CT scans within a short period. Third, we used high resolution MDCT (1 mm) as the reference; however, this modality may not be the ideal one. Finally, we only analyzed MDCT scans using a bone reconstruction algorithm, with no evaluation of the soft tissues. We did not check the soft tissue lesions which could be overlooked on CBCT.

5 | CONCLUSION

The CBCT with submillimeter thickness showed similar diagnostic capability to MDCT with 1 mm slice and superior performance to MDCT with 3 mm slice. Considering its low radiation dose, low cost, and ease of clinical access, CBCT may be a useful imaging modality

for as first line sinonasal evaluation and repeated follow up. However, its limitations in assessing soft tissue structures and precise preoperative planning, due to low soft-tissue contrast resolution, increased noise levels, low SNR and low CNR values, should be considered.

CONFLICT OF INTEREST

The authors declare that they have no conflict of interest.

AUTHOR CONTRIBUTIONS

Hyun Jun Kim designed the study and finally approved the article. Miran Han drafted and revising the manuscript. Miran Han and Hyun Jun Kim analyzed and interpreted the data. Jin Wook Choi, Do-Yang Park, and Jang Gyu Han collected the data.

ETHICS STATEMENT

This study was approved by our Institutional Review Board (Ajou Institutional Review Board, AJIRB-MED-MDB-20-149) and the requirement for written informed consent was waived due to its retrospective nature.

DATA AVAILABILITY STATEMENT

The data that support the findings of this study are available from the corresponding author upon reasonable request.

ORCID

Miran Han https://orcid.org/0000-0001-7752-5858
Hyun Jun Kim https://orcid.org/0000-0002-3134-0142

REFERENCES

1. Robb RA. The dynamic spatial reconstructor: an x-ray video-fluoroscopic CT scanner for dynamic volume imaging of moving organs. *IEEE Trans med Imaging*. 1982;1:22-33.
2. Cho PS, Johnson RH, Griffin TW. Cone-beam CT for radiotherapy applications. *Phys Med Biol*. 1995;40:1863-1883.
3. Daly MJ, Siewerdsen JH, Moseley DJ, Jaffray DA, Irish JC. Intraoperative cone-beam CT for guidance of head and neck surgery: assessment of dose and image quality using a C-arm prototype. *Med Phys*. 2006;33:3767-3780.
4. Rafferty MA, Siewerdsen JH, Chan Y, et al. Intraoperative cone-beam CT for guidance of temporal bone surgery. *Otolaryngol Head Neck Surg*. 2006;134:801-808.
5. Hodez C, Griffaton-Taillandier C, Bensimon I. Cone-beam imaging: applications in ENT. *Eur Ann Otorhinolaryngol Head Neck Dis*. 2011; 128:65-78.
6. Dahmani-Causse M, Marx M, Deguine O, Fraysse B, Lepage B, Escude B. Morphologic examination of the temporal bone by cone beam computed tomography: comparison with multislice helical computed tomography. *Eur Ann Otorhinolaryngol Head Neck Dis*. 2011; 128:230-235.
7. Robotti E, Daniel RK, Leone F. Cone-beam computed tomography: a user-friendly, practical roadmap to the planning and execution of every rhinoplasty—a 5-year review. *Plast Reconstr Surg*. 2021;147: 749e-762e.
8. Özeren Keşkek C, Aytuğar E. Radiological evaluation of olfactory fossa with cone-beam computed tomography. *J Oral Maxillofac Res*. 2021;12:e3.
9. Nikkerdar N, Eivazi N, Lotfi M, Golshah A. Agreement between cone-beam computed tomography and functional endoscopic sinus surgery for detection of pathologies and anatomical variations of the paranasal sinuses in chronic rhinosinusitis patients: a prospective study. *Imaging Sci Dent*. 2020;50:299-307.
10. Cakli H, Cingi C, Ay Y, Oghan F, Ozer T, Kaya E. Use of cone beam computed tomography in otolaryngologic treatments. *Eur Arch Otorhino-laryngol*. 2012;269:711-720.
11. Scarfe WC, Farman AG. What is cone-beam CT and how does it work? *Dent Clin N Am*. 2008;52:707-730, v.
12. Miracle AC, Mukherji SK. Conebeam CT of the head and neck, part 1: physical principles. *AJNR Am J Neuroradiol*. 2009;30:1088-1095.
13. Ludlow JB, Ivanovic M. Comparative dosimetry of dental CBCT devices and 64-slice CT for oral and maxillofacial radiology. *Oral Surg Oral Med Oral Pathol Oral Radiol Endod*. 2008;106:106-114.
14. Al Abduwani J, ZilinSkiene L, Colley S, Ahmed S. Cone beam CT paranasal sinuses versus standard multidetector and low dose multidetector CT studies. *Am J Otolaryngol*. 2016;37:59-64.
15. Suomalainen A, Kiljunen T, Kaser Y, Peltola J, Kortesniemi M. Dosimetry and image quality of four dental cone beam computed tomography scanners compared with multislice computed tomography scanners. *Dentomaxillofac Radiol*. 2009;38:367-378.
16. Peter M, Som HC. *Head and Neck Imaging*. Mosby; 2011.
17. Melhem ER, Oliverio PJ, Benson ML, Leopold DA, Zinreich SJ. Optimal CT evaluation for functional endoscopic sinus surgery. *Am J Neuroradiol*. 1996;17:181-188.
18. Rao VM, el-Noueam KI. Sinonasal imaging: anatomy and pathology. *Radiol Clin North Am*. 1998;36:921-939, vi.
19. Kirsch CFE, Bykowski J, Aulino JM, et al. ACR Appropriateness Criteria(®) sinonasal disease. *J Am Coll Radiol*. 2017;14:S550-s559.
20. Miracle AC, Mukherji SK. Conebeam CT of the head and neck, part 2: clinical applications. *AJNR Am J Neuroradiol*. 2009;30:1285-1292.
21. Tao S, Rajendran K, Zhou W, Fletcher JG, McCollough CH, Leng S. Noise reduction in CT image using prior knowledge aware iterative denoising. *Phys Med Biol*. 2020;65(22). doi:10.1088/1361-6560/abc231
22. Demeslay J, Vergez S, Serrano E, et al. Morphological concordance between CBCT and MDCT: a paranasal sinus-imaging anatomical study. *Surg Radiol Anat*. 2016;38:71-78.
23. Fakhran S, Alhilali L, Sreedher G, et al. Comparison of simulated cone beam computed tomography to conventional helical computed tomography for imaging of rhinosinusitis. *Laryngoscope*. 2014;124: 2002-2006.
24. De Cock J, Zanca F, Canning J, Pauwels R, Hermans R. A comparative study for image quality and radiation dose of a cone beam computed tomography scanner and a multislice computed tomography scanner for paranasal sinus imaging. *Eur Radiol*. 2015;25:1891-1900.
25. Sharma GK, Foulad A, Shamouelian D, Bhandarkar ND. Inefficiencies in computed tomography sinus imaging for management of sinonasal disease. *Otolaryngol Head Neck Surg*. 2017;156:575-582.
26. Huang BY, Senior BA, Castillo M. Current trends in sinonasal imaging. *Neuroimaging Clin N Am*. 2015;25:507-525.
27. Lofthag-Hansen S, Thilander-Klang A, Ekestubbe A, Helmrot E, Gröndahl K. Calculating effective dose on a cone beam computed tomography device: 3D Accuitomo and 3D Accuitomo FPD. *Dentomaxillofac Radiol*. 2008;37:72-79.
28. Protection RJEBG. *Cone Beam CT for Dental and Maxillofacial Radiology*; 2011.
29. Ludlow JB, Timothy R, Walker C, et al. Effective dose of dental CBCT—a meta analysis of published data and additional data for nine CBCT units. *Dentomaxillofac Radiol*. 2015;44:20140197.

30. Leiva-Salinas C, Flors L, Gras P, et al. Dental flat panel conebeam CT in the evaluation of patients with inflammatory sinonasal disease: diagnostic efficacy and radiation dose savings. *AJNR Am J Neuroradiol*. 2014;35:2052-2057.

31. Protection RJAI. *ICRP Publication 103*; 2007;37:2.

32. Earwaker J. Anatomic variants in sinonasal CT. *Radiographics*. 1993; 13:381-415.

33. Kantarci M, Karasen RM, Alper F, Onbas O, Okur A, Karaman A. Remarkable anatomic variations in paranasal sinus region and their clinical importance. *Eur J Radiol*. 2004;50:296-302.

34. Kundel HL, Polansky M. Measurement of observer agreement. *Radiology*. 2003;228:303-308.

35. Landis JR, Koch GG. The measurement of observer agreement for categorical data. *Biometrics*. 1977;33:159-174.

36. Epstein VA, Kern RC. Invasive fungal sinusitis and complications of rhinosinusitis. *Otolaryngol Clin North Am*. 2008;41:497-524, viii.

37. Ziegler A, Patadia M, Stankiewicz J. Neurological complications of acute and chronic sinusitis. *Curr Neurol Neurosci Rep*. 2018;18:5.

38. Wu EL, Riley CA, Hsieh MC, Marino MJ, Wu XC, McCoul ED. Chronic sinonasal tract inflammation as a precursor to nasopharyngeal carcinoma and sinonasal malignancy in the United States. *Int Forum Allergy Rhinol*. 2017;7:786-793.

39. Brisco J, Fuller K, Lee N, Andrew D. Cone beam computed tomography for imaging orbital trauma—image quality and radiation dose compared with conventional multislice computed tomography. *Br J Oral Maxillofac Surg*. 2014;52:76-80.

40. Brenner DJ, Hall EJ. Computed tomography—an increasing source of radiation exposure. *N Engl J Med*. 2007;357:2277-2284.

41. Christell H, Birch S, Horner K, Rohlin M, Lindh C. A framework for costing diagnostic methods in oral health care: an application comparing a new imaging technology with the conventional approach for maxillary canines with eruption disturbances. *Community Dent Oral Epidemiol*. 2012;40:351-361.

42. Leung R, Kern R, Jordan N, et al. Upfront computed tomography scanning is more cost-beneficial than empiric medical therapy in the initial management of chronic rhinosinusitis. *Int Forum Allergy Rhinol*. 2011;1:471-480.

43. Leung RM, Chandra RK, Kern RC, Conley DB, Tan BK. Primary care and upfront computed tomography scanning in the diagnosis of chronic rhinosinusitis: a cost-based decision analysis. *Laryngoscope*. 2014;124:12-18.

44. Friedland B. Medicolegal issues related to cone beam CT. *Semin Orthod*. 2009;15(1):77-84.

45. Pauwels R, Beinsberger J, Stamatakis H, et al. Comparison of spatial and contrast resolution for cone-beam computed tomography scanners. *Oral Surg Oral Med Oral Pathol Oral Radiol*. 2012;114:127-135.

46. Setzen G, Ferguson BJ, Han JK, et al. Clinical consensus statement: appropriate use of computed tomography for paranasal sinus disease. *Otolaryngology*. 2012;147:808-816.